Publishing Excellence
Inspiring Progress
ARISTON PUBLICATIONS
Quantum Advances
ISSN: 3143-0724 www.aristonpubs.com/journal/quantum-advances https://doi.org/10.69626/qa.2026.0046

RESEARCH ARTICLE

Combined Effects of Impurity Ionization and Transverse Electric Fields on the Electronic Structure of Double Quantum Wells

V. Akimov[1*], R. Demediuk[2], O. Miezientseva[2]

ABSTRACT: In this work we investigate theorically the influence of thermal ionization of donor impurities in a δ-doped layer and a transverse electric field on the energy levels and intersubband absorption in a Si double quantum well with $Si_{0.8}Ge_{0.2}$ barriers. Charge redistribution modifies the potential profile, altering the energies and spacing of size-quantization levels and, consequently, the absorption spectra. Compared with a single quantum well, the double quantum well exhibits better-resolved absorption peaks. These results demonstrate an effective approach for tuning the optical response and frequency of silicon-based terahertz optoelectronic devices.

Keywords: Double Quantum Wells; Modulation Doping; Terahertz; Silicon-germanium Heterostructures; Impurity Ionization; Optical Transitions

Received: 24 April 2026; Revised: 02 May 2026; Accepted: 13 May 2026; Published Online: 01 June 2026

1. INTRODUCTION

Intersubband transitions in semiconductor quantum wells (QWs) in optoelectronic devices, including Quantum Cascade Lasers (QCLs) [1–3] and Quantum Well Infrared Photodetectors (QWIPs) [4–7], constitute an important research area at the intersection of condensed matter physics, photonics, and semiconductor device engineering. These devices operate predominantly in the mid-to-far-infrared and terahertz (THz) spectral regions and have found numerous applications in spectroscopy, chemical sensing, free-space communications, medical diagnostics, security screening, environmental monitoring, and imaging. Their performance strongly depends on the energy separation between quantized electronic subbands, which determines the emission or absorption wavelength One of the principal challenges in the development of intersubband optoelectronic devices is achieving efficient frequency tunability without modifying the heterostructure itself. Unlike interband devices, where the emission wavelength can often be adjusted through material composition or carrier injection, the operating frequency of intersubband devices is primarily governed by the quantum confinement potential. Consequently, the ability to dynamically manipulate subband energies by external means has attracted considerable interest. Various approaches have been proposed, including external electric fields (Quantum Confined Stark Effect) [8, 9], electrostatic gating [10, 11], strain engineering [12, 13], magnetic fields [14, 15], and modifications of the carrier distribution within the quantum well [16, 17]. Developing new tuning mechanisms compatible with silicon technology remains particularly important for future CMOS-compatible THz photonics.

In our work [18], we demonstrated that thermal ionization of donors in a δ-doped layer provides an effective mechanism for controlling the electronic

[1] Instituto de Ciencias Básicas, Universidad de Medellín, Carrera 87 No. 30–65, Medellín 050026, Colombia.

[2] Department of Mathematics, Physics and Computer Science, Donbas State Pedagogical University, 19 Henerala Batiuka St., Sloviansk, Donetsk Oblast 84116, Ukraine.

[*] Author to whom correspondence should be addressed: intremun@gmail.com (V. Akimov)

© Ariston Publications 2026. All rights reserved.

spectrum of a semiconductor quantum well. As the electronic temperature increases, a larger fraction of donor atoms becomes ionized, leading simultaneously to an increase in the electron concentration occupying the quantized states of the well and to the accumulation of positively charged donor ions within the δ-layer. This charge redistribution modifies the self-consistent electrostatic potential by superimposing a narrow V-shaped perturbation on the original rectangular confinement profile existing at low temperature. As the perturbation becomes deeper, additional localized states appear inside the modified potential. Owing to the narrower spatial extent of the V-shaped potential, the spacing between these newly formed quantized levels is considerably larger than that associated with the original rectangular well. Since the lowest subbands accommodate most of the electron population, the resulting modification of their energy separation produces a shift of the intersubband transition frequency reaching several terahertz. The present work extends this concept to a double quantum well (DQW) heterostructure containing a δ-doped layer positioned near one edge of one of the wells. In comparison with a single quantum well, coupled quantum wells provide an additional degree of freedom arising from wavefunction hybridization and tunneling between adjacent wells. These effects increase the sensitivity of the electronic spectrum to changes in the confinement potential and external perturbations, thereby offering the possibility of a substantially broader frequency tuning range. Furthermore, the interaction between symmetric and antisymmetric electronic states in coupled wells is expected to improve spectral selectivity by producing better-separated intersubband absorption peaks.

It should be emphasized that the temperature considered throughout this work is the electronic temperature, which characterizes the energy distribution of the electron gas and does not necessarily coincide with the lattice temperature. Electronic temperature can be modified not only by varying the ambient temperature but also through optical excitation, electrical injection, or high-field transport. Consequently, it can be regarded as an independent control parameter that complements the externally applied transverse electric field for tailoring the electronic properties of the heterostructure. The objective of this work is to provide a quantitative and qualitative investigation of the combined influence of donor ionization in a δ-doped layer and an externally applied transverse electric field on the energy spectrum and intersubband optical transitions in Si/SiGe double quantum wells. Particular attention is devoted to evaluating the achievable tuning range of the lowest size-quantization levels and the corresponding absorption frequencies. The proposed tuning mechanism offers a promising route toward dynamically reconfigurable silicon-based THz and mid-infrared optoelectronic devices, including quantum cascade lasers, photodetectors, optical modulators, and integrated photonic components.

2. THEORETICAL MODEL

The heterostructure investigated in this work is a silicon-based double quantum well (DQW) comprising two Si quantum wells separated and confined by $Si_{0.8}Ge_{0.2}$ barrier layers. A phosphorus δ-doped layer is positioned at the edge of one of the quantum wells, as illustrated in Figure 1. This asymmetric doping configuration enables redistribution of the electron charge under donor ionization and enhances the sensitivity of the electronic states to external perturbations, such as an applied transverse electric field.

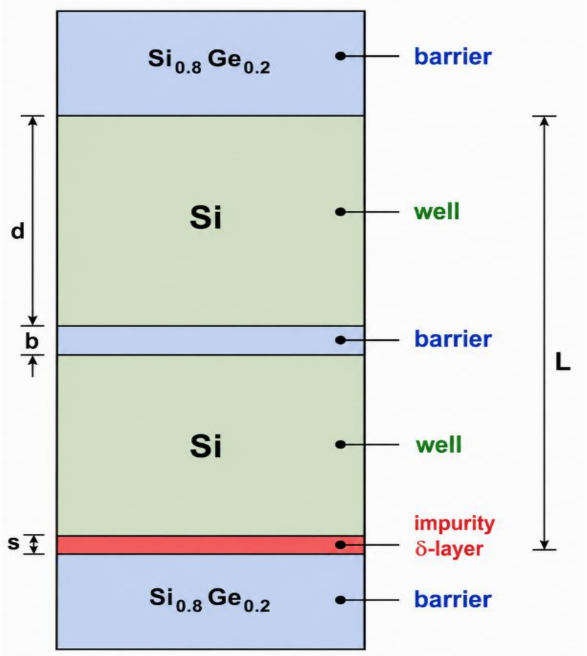


Fig. 1. One period of the heterostructure under study.

Each quantum well has a width of $d = 10$ nm, while the barrier separating the adjacent wells has a thickness of $b = 2$ nm. The δ-doped phosphorus layer has a finite thickness of $s = 1$ nm. Accordingly, the total width of the coupled double quantum well region is $L = 2d + b = 22$ nm. The sheet concentration of phosphorus donors is $n_d = 1.2 \times 10^{12}$ cm^{-2}, which provides a sufficient electron density for the observation of pronounced intersubband transitions while maintaining strong quantum confinement. The selected structural

© Ariston Publications 2026. All rights reserved.

parameters are representative of experimentally realizable Si/SiGe heterostructures and ensure efficient coupling between the two wells, making the structure well suited for investigating the combined effects of donor ionization and externally applied electric fields on the electronic energy spectrum and intersubband optical properties. To investigate the proposed tuning mechanism, a self-consistent numerical model was developed based on the iterative solution of the coupled Schrödinger, Poisson, and electroneutrality equations. This approach enables simultaneous determination of the electronic states, electrostatic potential, and charge distribution, while accounting for the mutual interaction between the confined electrons and ionized donor impurities. The iterative procedure continues until convergence is achieved for both the potential profile and the electronic energy spectrum.

A key parameter governing the electron redistribution is the impurity binding energy (IBE), which determines the degree of donor ionization and, consequently, the concentration of free carriers in the quantum wells. In many theoretical studies of doped semiconductor heterostructures, the IBE is assumed to be equal to its bulk-material value and independent of the local electrostatic environment. Such an approximation is not appropriate for the present structure because the donor impurities are confined to a δ-doped layer located near the quantum-well edge, where quantum confinement, dielectric mismatch, and band bending significantly modify the impurity potential. As a result, the impurity binding energy becomes strongly dependent on the self-consistent potential profile and cannot be treated as a fixed parameter.

To account for these effects, the impurity binding energy was calculated at each iteration using the method proposed in [19]. The resulting value was then incorporated into the electroneutrality condition to determine the donor ionization degree and the corresponding free-electron concentration. This procedure allows the redistribution of charge between the δ-doped layer and the quantum wells to be described self-consistently, providing an accurate representation of the temperature- and electric-field-dependent potential profile.

Within the effective-mass approximation, the electronic states were obtained by solving the one-dimensional stationary Schrödinger equation for the Hamiltonian

$$H = -\frac{\hbar^2}{2m_\perp}\frac{d^2}{dz^2} + V(z) + e\phi(z) + eFz \tag{1}$$

The first term in the Hamiltonian represents the kinetic energy of an electron within the effective-mass approximation. Here, z denotes the growth direction of the heterostructure, which is perpendicular to the quantum-well layers, and $m_\perp$ is the corresponding electron effective mass along this direction. Since the electron motion is confined only along the growth axis, the problem is reduced to a one-dimensional quantum-mechanical description.

The second term, $V(z)$, represents the conduction-band confinement potential of the heterostructure. It is determined by the conduction-band offset between the Si quantum wells and the $Si_{0.8}Ge_{0.2}$ barrier layers and therefore defines the rectangular double quantum well profile in the absence of free-carrier redistribution and external perturbations.

The third term corresponds to the self-consistent Hartree (electrostatic) potential, $\phi(z)$, arising from the spatial redistribution of electrons and ionized donor impurities. As donor atoms in the δ-doped layer become ionized, the resulting separation of positive and negative charges modifies the electrostatic potential inside the heterostructure. This redistribution produces a localized V-shaped perturbation superimposed on the original rectangular confinement potential. The depth and spatial extent of this perturbation depend on the degree of donor ionization and therefore vary with the electronic temperature and the external electric field. Consequently, the Hartree potential plays a crucial role in determining the energies, spacing, and localization of the size-quantized electronic states.

The final term describes the interaction of the confined electrons with the externally applied transverse electric field, F. The electric field tilts the overall confinement potential, breaking the structural symmetry of the double quantum well and shifting the electron wavefunctions toward one side of the heterostructure. In combination with the Hartree potential, this effect provides an additional mechanism for controlling the energy spectrum and intersubband transition energies, thereby enabling dynamic tuning of the optical response of the structure.

$$V(z) = \begin{cases} V_b, & |z| \geq d + \frac{b}{2} \text{ or } |z| < \frac{b}{2} \\ 0, & d + \frac{b}{2} > |z| \geq \frac{b}{2} \end{cases} \tag{2}$$

where V_b is the conduction-band offset between the Si quantum wells and the $Si_{0.8}Ge_{0.2}$ barrier layers, which determines the depth of the quantum confinement potential. The origin of the coordinate system ($z = 0$) is chosen at the center of the barrier separating the two quantum wells, so that the heterostructure geometry is conveniently described

 © Ariston Publications 2026. All rights reserved.

with respect to the middle of the coupled double-well system.

The Fermi level, used below is determined from the electroneutrality condition

$$\int_{-\infty}^{\infty} n_c(z)\, dz = 0 \tag{3}$$

which ensures overall electrical neutrality of the heterostructure. Here, n_c denotes the net volumetric charge density, defined as the difference between the concentrations of positively charged ionized donors and negatively charged free electrons. Since both quantities depend on the electronic energy spectrum and the Fermi level, Eq. (3) must be solved simultaneously with the Schrödinger and Poisson equations within the iterative self-consistent procedure.

The electrostatic (Hartree) potential, $\phi(z)$, is obtained by direct integration of the one-dimensional Poisson equation.

$$\frac{d^2\phi}{dz^2} = \frac{e}{\varepsilon\varepsilon_0} n_c(z) \tag{4}$$

Here, ε_0 is the vacuum permittivity, while ε denotes the relative dielectric permittivity of the semiconductor material. In the calculations, the dielectric constants were taken as $\varepsilon = 11.7$ for the Si quantum wells and $\varepsilon = 12.6$ for the $Si_{0.8}Ge_{0.2}$ barrier layers. These values determine the electrostatic screening and, consequently, influence the self-consistent Hartree potential arising from the spatial redistribution of charge within the heterostructure.

The Hartree potential accounts for the Coulomb interaction between the spatially separated free electrons and ionized donor impurities and therefore describes the modification of the confinement potential caused by charge redistribution. Its self-consistent inclusion is essential for accurately predicting the electronic structure, particularly under conditions of partial donor ionization and in the presence of an externally applied transverse electric field, where significant changes in the potential profile and the corresponding size-quantized energy levels may occur.

The intersubband optical absorption coefficient was evaluated within the electric-dipole approximation using Fermi's golden rule. To account for the finite lifetime of the electronic states and scattering-induced broadening, the Dirac delta function describing energy conservation was replaced by a Lorentzian line-shape function. Assuming thermal equilibrium of the electron gas, the absorption coefficient was calculated following the approach described in [20]:

$$\alpha(E) = \frac{E\mu_0 ce^2}{\hbar n} \sum_{i,f} \frac{|M_{if}|^2 \sigma_{ij}}{\Gamma + \frac{(E_f - E_i - E)^2}{\Gamma}} \tag{5}$$

where $E = \hbar\omega$ is the is the incident photon energy, μ_0 vacuum permeability, c is the speed of light in vacuum, and n is the refractive index of the material. The quantities E_i and E_f represent the energies of the initial and final size-quantized subbands, respectively, obtained from the self-consistent solution of the stationary Schrödinger equation. The parameter Γ is the phenomenological linewidth (broadening parameter), which accounts for finite carrier lifetime and various scattering mechanisms, including impurity, interface roughness, and phonon scattering.

The equilibrium population difference between the participating subbands is given by

$$\sigma_{if} = \frac{m_{\|} k_b T}{L\pi\hbar^2} \ln\left(\frac{e^{\frac{E_F - E_i}{k_b T}} + 1}{e^{\frac{E_F - E_f}{k_b T}} + 1} \right) \tag{6}$$

where k_b is the Boltzmann constant, T is the electronic temperature, E_F is the Fermi energy determined from the self-consistent solution of the electroneutrality equation, and $m_{\|}$ is the electron effective mass in the plane of the quantum wells. The quantity σ_{if} reflects the difference in the occupation probabilities of the initial and final subbands and therefore determines the strength of the corresponding intersubband absorption.

The optical transition matrix elements were calculated within the dipole approximation as

$$M_{if} = \int \psi_i^*(z)\, z\, \psi_f(z)\, dz \tag{7}$$

where $\psi_i^*(z)$ and $\psi_f(z)$ are the envelope wavefunctions of the corresponding size-quantized states. The magnitude of M_{if} determines the oscillator strength of the optical transition and depends on the spatial overlap and parity of the electron wavefunctions. Consequently, any modification of the confinement potential due to donor ionization or an externally applied transverse electric field affects not only the subband energies but also the transition probabilities through changes in the wavefunction localization and overlap.

Unless otherwise stated, all material parameters used in the numerical calculations, including the effective masses, dielectric constants, band offsets, and other physical constants, were adopted from [21].

© Ariston Publications 2026. All rights reserved.

3. RESULTS AND DISCUSSION

Figure 2 presents the calculated self-consistent potential profiles, the first four size-quantized energy levels, and the corresponding squared envelope wavefunctions for four electronic temperatures. The total confinement potential shown in the figure is obtained as the sum of the last three terms in the Hamiltonian (Eq. 1), namely the rectangular heterostructure potential, the self-consistent Hartree potential resulting from charge redistribution, and the potential associated with the externally applied transverse electric field. The squared wavefunctions represent the spatial probability density of electrons occupying the corresponding quantized states and therefore describe the distribution of the negative charge entering the electroneutrality condition (Eq. 3). In contrast, the positive charge is localized entirely within the phosphorus δ-doped layer, whose position is indicated by the short red horizontal line corresponding to the energy of the donor ground state.

As the electronic temperature increases, a larger fraction of donor impurities becomes thermally ionized, resulting in a simultaneous increase in the concentration of free electrons confined in the quantum wells and positively charged donor ions remaining in the δ-layer (Table 1, n_d). This enhanced charge separation strengthens the internal electrostatic field and significantly modifies the self-consistent potential profile. Instead of the nearly rectangular confinement potential observed at low temperatures, an additional localized V-shaped electrostatic perturbation develops in the vicinity of the δ-doped layer. The depth of this perturbation increases with the donor ionization degree, thereby producing progressively stronger localization of the electronic states.

As the V-shaped potential becomes deeper, it supports additional localized quantum states whose spatial localization differs from that of the states associated with the original rectangular double quantum well. Because the electrostatic perturbation is considerably narrower than the geometrical width of the quantum wells, the corresponding confinement is stronger, resulting in an increased energy separation between neighboring size-quantized levels. This effect is particularly pronounced for the lowest electronic states, which accommodate the majority of the electrons and therefore dominate the intersubband optical response. Consequently, the spacing between the first and second subbands exhibits a pronounced dependence on the electronic temperature. The calculated results shown in Figure 2 and summarized in Table 1 demonstrate that

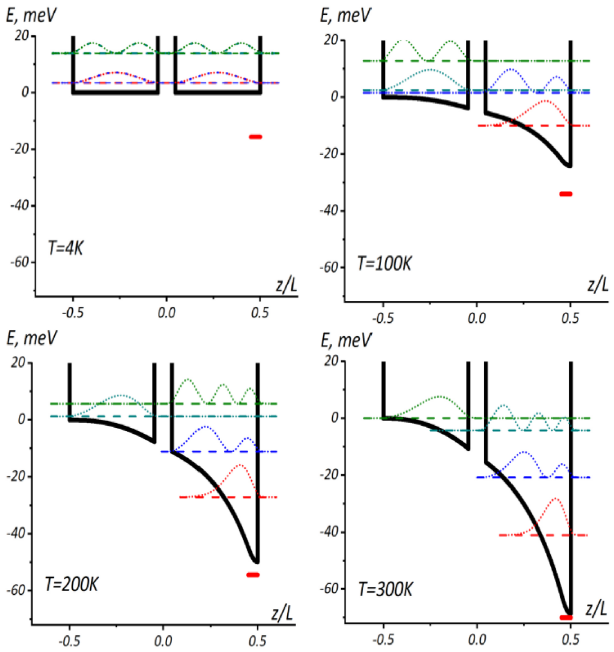


Fig. 2. Potential profile (solid black line), positions of the first four size-quantization levels (dotted lines), and squares of the corresponding wave functions (dashed lines) at temperatures 4, 100, 200 and 300K. F=0.

thermal ionization of donor impurities provides an efficient mechanism for controlling the electronic spectrum of $Si/Si_{0.8}Ge_{0.2}$ double quantum wells. The temperature-induced redistribution of charge modifies the self-consistent confinement potential, leading to systematic shifts of the quantized energy levels and changes in their mutual separation. Since the energies of intersubband optical transitions are directly determined by these level spacings, the observed effect offers a practical means of tuning the absorption and emission frequencies of the heterostructure. These findings confirm that donor ionization can serve as an effective internal control mechanism for engineering the electronic and optical properties of δ-doped Si/SiGe double quantum wells without altering their structural parameters.

The calculations show that the energy separation between the first and second size-quantized subbands changes by approximately 20 meV over the investigated electronic temperature range (Table 1, E_{12}). This variation corresponds to a shift of the intersubband transition frequency of about 5 THz, demonstrating that thermal ionization of the δ-doped donors provides an effective mechanism for dynamically tuning the optical response of the heterostructure. Since the lowest two subbands possess the highest electron occupation probability, this transition is expected to dominate the intersubband absorption spectrum and is therefore of primary importance for terahertz optoelectronic applications.

 © Ariston Publications 2026. All rights reserved.

Table 1. Energies for the transitions 1-2, 2-3 and 3-4 (E_{12}, E_{23}, E_{34}), impurity binding energy (E_δ), and impurity ionization degree (n_d) for different temperatures at $F = 0$.

T (K)	E_{12} (meV)	E_{23} (meV)	E_{34} (meV)	E_δ (meV)	n_d (%)
0	0.0	10.4	0.0	19.1	0
50	4.4	6.1	4.3	20.9	6
100	11.5	0.9	10.3	24.1	21
150	13.7	6.9	9.9	26.1	36
200	16.0	12.4	4.4	27.3	49
250	18.2	16.7	0.1	27.8	59
300	20.2	17.1	3.8	28.9	66

A more complex behavior is observed for the energy separation between the second and third subbands (Table 1, E_{23}). In contrast to the monotonic increase of E_{12}, the spacing E_{32} initially decreases with increasing temperature, reaches a minimum at approximately 100 K, and subsequently begins to increase. This non-monotonic behavior originates from the evolution of the self-consistent confinement potential. As the electronic temperature rises, the increasing concentration of ionized donors deepens the V-shaped Hartree perturbation. At relatively low temperatures, the ground-state wavefunction becomes localized within this electrostatic well, while the second subband is displaced toward the remaining part of the rectangular quantum-well potential. Consequently, the energy separation between the second and third levels decreases for the initial stage of donor ionization. When the electronic temperature reaches approximately 100-150 K, the V-shaped perturbation becomes sufficiently deep to confine the second subband as well. From this point onward, both the first and second subbands experience stronger confinement within the narrow electrostatic potential, causing the energy separation E_{23} to increase with further temperature. This behavior illustrates the gradual restructuring of the electronic spectrum driven by the temperature-dependent modification of the self-consistent potential profile.

Interestingly, the energy separation E_{34} approaches zero at approximately $T = 250$ K. This behavior results from a reordering of the energy levels. At low temperatures, the third subband is primarily localized in the left-hand quantum well. As the temperature increases, charge redistribution deepens the right-hand potential well, causing one of its confined states to shift downward in energy. Eventually, this state drops below the original third subband and becomes the new third energy level, leading to an anticrossing-like reordering of the spectrum (see Figure 2). The calculated impurity binding energy also exhibits a systematic dependence on the electronic temperature (Table 1, E_δ). As the temperature increases, the impurity binding energy gradually becomes larger, reflecting the continuous evolution of the electrostatic environment surrounding the donor atoms. This behavior is consistent with the strengthening of the Hartree potential produced by charge redistribution between the δ-doped layer and the quantum wells. Since the impurity binding energy determines the degree of donor ionization, its self-consistent variation further reinforces the redistribution process and contributes to the modification of the confinement potential.

Overall, these results demonstrate that thermally induced donor ionization produces substantial and controllable changes in the electronic spectrum of the $Si/Si_{0.8}Ge_{0.2}$ double quantum well. Unlike conventional methods that require modifications of the heterostructure geometry or composition, the proposed mechanism exploits internal charge redistribution to alter the energy spacing between quantized states. This approach enables reversible tuning of intersubband transition energies and, consequently, of the operating frequency of terahertz to mid-infrared optoelectronic devices while preserving the original structural design of the heterostructure.

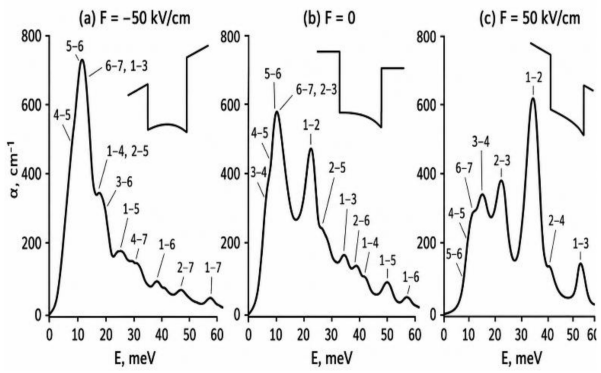


Fig. 3. Absorption spectra of intersubband transitions for single QW: (a) F=-50kV/cm; (b) F=0; (c) F=50kV/cm; T=300 K. In the insets are energy profiles.

Figure 3 and 4 compare the calculated intersubband absorption spectra, expressed in absolute units (cm^{-1}), for two heterostructure configurations: a double quantum well (Figure 4) containing a thin internal barrier and a single quantum well (Figure 3) with identical structural parameters except for the absence of the central barrier ($b = 0$). The spectra are presented for three values of the externally applied transverse electric field. All spectra are plotted using identical horizontal and vertical scales to facilitate direct comparison, and the most important intersubband transitions are identified in each panel.

© Ariston Publications 2026. All rights reserved.

The sign of the electric field determines the direction in which the confinement potential is tilted. A positive electric field ($F > 0$) inclines the potential toward the right-hand side of the structure, reinforcing the electrostatic well created by the positively charged ionized donors. Consequently, the V-shaped perturbation becomes deeper and narrower, producing stronger localization of the lowest electronic states and increasing the separation between the lowest subbands. In contrast, a negative electric field ($F < 0$) tilts the potential in the opposite direction, partially compensating the electrostatic perturbation produced by the ionized donors. The overall confinement profile therefore becomes more symmetric, reducing the localization of the lowest states within the electrostatic well.

This qualitative symmetry has a pronounced influence on the optical transition probabilities. For $F = -50$ kV/cm, the first and second electronic states become predominantly localized on opposite sides of the heterostructure. Their spatial overlap is therefore substantially reduced, resulting in very small dipole matrix elements and, consequently, strongly suppressed $1 \rightarrow 2$ absorption peaks in both the SQW and DQW structures. This observation clearly demonstrates that the external electric field affects not only the transition energies but also the oscillator strengths through modifications of the wavefunction localization.

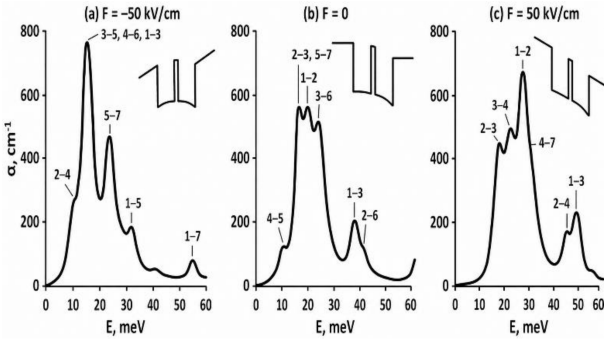


Fig. 4. Absorption spectra of intersubband transitions for double QW: (a) F=-50kV/cm; (b) F=0; (c) F=50kV/cm; T=300 K. In the insets are energy profiles.

At room electronic temperature, thermal population extends beyond the lowest subbands, with a significant number of electrons occupying states up to the fourth subband. Consequently, transitions originating from higher-energy states also contribute to the absorption spectrum. Depending on the applied electric field, these transitions may generate distinct absorption peaks, as illustrated by the $4 \rightarrow 5$ transition in Figure 4b, or modify the line shape of stronger transitions through spectral overlap, as observed for the $4 \rightarrow 7$ transition in Figure 4c. The resulting spectrum contains numerous partially overlapping resonances, which is a common characteristic of quantum-well structures with relatively small intersubband energy separations. Such spectral congestion complicates the realization of frequency-selective tunable devices because individual transitions become increasingly difficult to isolate.

A comparison between the single and double quantum well structures reveals one of the principal advantages of introducing a thin central barrier. Although the DQW preserves the strongest absorption maxima, many weaker transitions become significantly suppressed, yielding a considerably cleaner and better-resolved spectrum. This behavior can be attributed to the localization of the electronic wavefunctions within either the left or the right quantum well. Since many pairs of subbands are spatially separated, their overlap integrals decrease, reducing the corresponding dipole matrix elements and suppressing transitions that would otherwise contribute to spectral background. Consequently, the DQW configuration exhibits improved spectral selectivity compared with the SQW while maintaining comparable absorption intensity for the dominant transitions.

The applied transverse electric field provides an additional means of controlling the spectral response. The most pronounced qualitative changes occur when the electric field is increased from 0 to $+50$ kV/cm. Under these conditions, the lower part of the confinement potential becomes effectively narrower due to the combined action of the electric field and the Hartree potential, increasing the spacing between the lowest subbands. As a result, the dominant absorption peaks shift toward higher photon energies. This blue shift is considerably more pronounced for the DQW than for the SQW because the coupled-well configuration is more sensitive to changes in the confinement potential. Although the SQW exhibits the same general trend, its spectrum contains a larger number of weaker peaks that partially obscure the shift of the dominant transitions. By contrast, changing the electric field from 0 to -50 kV/cm produces comparatively modest changes in the spectral distribution because the negative field partially compensates the electrostatic asymmetry introduced by the δ-doped layer instead of enhancing it.

Among the available tuning parameters, the transverse electric field represents the most practical and rapidly adjustable control mechanism, since it can be varied continuously during device operation without altering the carrier concentration or the heterostructure itself. This makes electric-field tuning particularly attractive for applications requiring

 © Ariston Publications 2026. All rights reserved.

dynamic control of intersubband transitions in the energy range of approximately 10-30 meV. The donor ionization degree also provides an effective tuning mechanism through its influence on the self-consistent potential profile; however, controlling the electronic temperature or nonequilibrium carrier distribution is experimentally more challenging. Moreover, under room-temperature equilibrium conditions the donor ionization degree is already close to its maximum value, so the associated spectral broadening and the presence of numerous higher-subband transitions cannot be significantly reduced. An alternative approach would be to employ narrower single quantum wells, which naturally support fewer confined states and therefore exhibit simpler absorption spectra. Nevertheless, such structures are less suitable for low-energy terahertz transitions and are expected to exhibit weaker sensitivity of the intersubband energies to externally applied electric fields. Consequently, the δ-doped double quantum well investigated here provides a favorable compromise between broad frequency tunability, low operating energies, and relatively high spectral selectivity, making it a promising platform for tunable silicon-based terahertz optoelectronic devices.

4. CONCLUSION

A self-consistent theoretical investigation of $Si/Si_{0.8}Ge_{0.2}$ double quantum wells containing a phosphorus δ-doped layer has demonstrated that the combined action of thermally induced donor ionization and an externally applied transverse electric field provides an effective mechanism for controlling the electronic energy spectrum. Charge redistribution between the δ-doped layer and the quantum wells modifies the self-consistent electrostatic potential, giving rise to a localized V-shaped perturbation that substantially alters the energies, spacing, and localization of the size-quantized electronic states. As a consequence, the energies of intersubband optical transitions can be tuned over a broad range without changing the structural parameters of the heterostructure.

The calculations show that thermal ionization of the donor impurities changes the energy separation between the lowest subbands by approximately 20 meV, corresponding to a frequency shift of about 5 THz. The application of a transverse electric field provides an additional independent tuning parameter, allowing further adjustment of both the transition energies and the oscillator strengths through modifications of the electron wavefunction localization. The combined use of these two control mechanisms enables continuous tuning of the terahertz absorption spectrum with a significant displacement of the dominant absorption peaks.

A comparison between single and double quantum well structures demonstrates that introducing a thin central barrier considerably improves the spectral characteristics. Although the strongest absorption peaks are preserved, many weaker transitions are suppressed because of reduced spatial overlap between the corresponding wavefunctions. Consequently, the double quantum well exhibits a cleaner and better-resolved absorption spectrum than a single quantum well of the same total width, facilitating selective tuning of the dominant intersubband transitions in the 10-40 meV energy range.

These results indicate that δ-doped Si/SiGe double quantum wells constitute a promising platform for dynamically tunable terahertz optoelectronic devices. The proposed tuning mechanism is fully compatible with silicon-based heterostructures and does not require modification of the device geometry, making it attractive for the development of reconfigurable quantum cascade emitters, photodetectors, optical modulators, and other integrated THz photonic components.

DECLARATIONS

Ethical Approval

We affirm that this manuscript is an original work, has not been previously published, and is not currently under consideration for publication in any other journal or conference proceedings. All authors have reviewed and approved the manuscript, and the order of authorship has been mutually agreed upon.

Funding

Funding not available

Availability of data and material

The datasets used and/or analyzed during the current study are available from the corresponding author on reasonable request.

Conflicts of Interest

The authors declare that they have no financial or personal interests that could have influenced the research and findings presented in this paper. The

© Ariston Publications 2026. All rights reserved.

authors alone are responsible for the content and writing of this article.

Authors' contributions

V. Akimov: Writing – Original draft, Supervision, Methodology; **R. Demediuk**: Investigation, Visualization; **O. Miezientseva**: Investigation, Software.

REFERENCES

[1] Faist, J., **2013**. Quantum Cascade Lasers. *Oxford University Press. https://academic.oup.com/book/3819*.

[2] Vitiello, M. S. and Tredicucci, A., **2021**. Physics and technology of terahertz quantum cascade lasers. *Advances in Physics: X*, 6(1), p.1893809. https://doi.org/10.1080/23746149.2021.1893809.

[3] Zheng, J.; Xu, D.; Wu, Q.; Zhang, C.; Lin, Y.; Yuan, M.; Qu, Y, **2025**. Research progress of single-mode quantum cascade lasers. *Coatings*, 15(8), p.950. https://doi.org/10.3390/coatings15080950.

[4] Rogalski, A., **2019**. Infrared and Terahertz Detectors. *CRC Press*. https://doi.org/10.1201/b21951.

[5] Schneider, H. and Liu, H. C., **2007**. Quantum Well Infrared Photodetectors: Physics and Applications. *Springer Series in Optical Sciences*, 126. https://shorturl.at/IXDLi.

[6] Shao, D. and Wang, Y. and Li, Z. and Zhang, Y. and Wang, L. and Liu, H., **2021**. Research progress on terahertz quantum-well photodetector and its application. *Frontiers in Physics*, 9, p.751018. https://doi.org/10.3389/fphy.2021.751018.

[7] Levine, B. F., **1993**. Quantum-well infrared photodetectors. *Journal of Applied Physics*, 74(8), p.R1-R81. https://doi.org/10.1063/1.354252.

[8] Bastard, G., **1988**. Wave Mechanics Applied to Semiconductor Heterostructures. *Les Editions de Physique. https://shorturl.at/uvuW3*.

[9] Miller, D. A. B. and Chemla, D. S. and Damen, T. C. and Gossard, A. C. and Wiegmann, W. and Wood, T. H. and Burrus, C. A., **1984**. Electric field dependence of optical absorption near the band gap of quantum-well structures. *Physical Review B*, 32(2), p.1043-1060. https://doi.org/10.1103/PhysRevB.32.1043.

[10] Ando, T. and Fowler, A. B. and Stern, F., **1982**. Electronic properties of two-dimensional systems. *Reviews of Modern Physics*, 54(2), p.437-672. https://doi.org/10.1103/RevModPhys.54.437.

[11] Davies, J. H., **1998**. The Physics of Low-Dimensional Semiconductors: An Introduction. *Cambridge University Press. https://shorturl.at/pFCPj*.

[12] Paul, D. J., **1999**. Silicon-germanium strained layer materials in microelectronics. *Advanced Materials*, 11(3), p.191-204. https://shorturl.at/20nPF.

[13] Li, H. and Wang, J. and Bai, J. and Zhang, S. and Zhang, S. and Sun, Y. and Dou, Q. and Ding, M. and Wang, Y. and Qu, D. and Du, J. and Tang, C. and Li, E. and Prades, J. D., **2020**. The structural, electronic, and optical properties of Ge/Si quantum wells: Lasing at a wavelength of 1550 nm. *Nanomaterials*, 10(5), p.1006. https://doi.org/10.3390/nano10051006.

[14] Scalari, G. and Walther, C. and Sirigu, L. and Sadowski, M. L., **2007**. Strong confinement in terahertz intersubband lasers by intense magnetic fields. *Physical Review B*, 76(11), p.115305. https://doi.org/10.1103/PhysRevB.76.115305.

[15] Apalkov, V. M. and Portnoi, M. E., **2002**. Tuning gaps and phases of a two-subband system in a quantizing magnetic field. *Physical Review B*, 65(12), p.125310. https://doi.org/10.1103/PhysRevB.65.125310.

[16] Hertle, H. and Schäffler, F. and Zrenner, A. and Abstreiter, G. and Gornik, E., **1992**. Electron intersubband absorption in modulation- and well-doped Si/Si1-xGex multiple quantum wells. *Thin Solid Films*, 222(1-2), p.20-23. https://doi.org/10.1016/0040-6090(92)90029-B.

[17] Paspalakis, E. and Boviatsis, J., **2012**. Ultrashort electromagnetic pulse control of intersubband quantum well transitions. *Nanoscale Research Letters*, 7, p.478. https://doi.org/10.1186/1556-276X-7-478.

[18] Tulupenko, V. N. and Duque, C. A. and Demedyuk, R., **2013**. On the possibility of tuning the energy separation between space-quantized levels in a quantum well. *Philosophical Magazine Letters*, 93(1), p.42-49. https://doi.org/10.1080/09500839.2012.729959.

 © Ariston Publications 2026. All rights reserved.

[19] Vinter, B., **1982**. Influence of charged impurities on Si inversion-layer electrons. *Physical Review B*, 26(12), p.6808-6817. https://doi.org/10.1103/PhysRevB.26.6808.

[20] Tulupenko, V. and Duque, C. A. and Akimov, V. and Demediuk, R., **2015**. On intersubband absorption of radiation in delta-doped QWs. *Physica E: Low-dimensional Systems and Nanostructures*, 74, p.400-406. https://doi.org/10.1016/j.physe.2015.07.034.

[21] Tulupenko, V. and Akimov, V. and Demediuk, R. and Tiutiunnyk, A. and Duque, C. A. and Sushchenko, D. and Fomina, O. and Morales, A. and Laroze, D., **2022**. Intersubband energy differences of delta-doped quantum wells in external electric field. *Proceedings of the IEEE 41st International Conference on Electronics and Nanotechnology (ELNANO)*, p.133-136. https://doi.org/10.1109/ELNANO54667.2022.9927043.

© Ariston Publications 2026. All rights reserved.